ARTICLES

Threshold electrodisintegration in the $A = 3$ system

G.A. Retzlaff, H. S. Caplan, E. L. Hallin, and D. M. Skopik
Saskatchewan Accelerator Laboratory, University of Saskatchewan, Saskatoon, Saskatchewan, Canada S7N 0W0

D. Beck,* K. I. Blomqvist,† G. Dodson, K. Dow, M. Farkhondeh, J. Flanz, S. Kowalski, W. W. Sapp, C. P. Sargent, D. Tieger, W. Turchinetz, and C. F. Williamson
Bates Linear Accelerator Center and Laboratory for Nuclear Science, Massachusetts Institute of Technology, Cambridge, Massachusetts 02139

W. Dodge,‡ X. K. Maruyama,§ and J. W. Lightbody, Jr.‖
National Institute of Standards and Technology, Gaithersburg, Maryland 20899

R. Goloskie
Department of Physics, Worcester Polytechnic Institute, Worcester, Massachusetts 01601

J. McCarthy, T. S. Ueng,¶ and R. R. Whitney**
Department of Physics, University of Virginia, Charlottesville, Virginia 22901

B. Quinn
Department of Physics, Carnegie-Mellon University, Pittsburgh, Pennsylvania 15213

S. Dytman and K. Von Reden††
Department of Physics, University of Pittsburgh, Pittsburgh, Pennsylvania 15260

R. Schiavilla
Instituto Nazionale di Fisica Nucleare, Lecce, Italy

J. A. Tjon
Institute for Nuclear Physics, University of Utrecht, 3508 TA Utrecht, The Netherlands

(Received 26 July 1993)

Inclusive inelastic electron scattering cross sections for ^{3}H and ^{3}He were measured for excitation energies below 18 MeV. Longitudinal and transverse response functions were determined from these cross sections for six values of the three-momentum transfer q in the range $0.88 < q < 2.87$ fm^{-1}. A previously observed $C0$ multipole enhancement near threshold in the two-body channel for ^{3}He is confirmed but is not observed for ^{3}H. The experimental data are found to be in good agreement with two recent calculations of the longitudinal and transverse response functions. The first uses variational ground-state wave functions and the orthogonal correlated states method to describe

*Present address: Department of Physics, University of Illinois, Urbana, IL 61801.
†Present address: Institute fur Kernphysik, Universitait Mainz, Germany.
‡Present address: George Washington University, Washington, D.C. 22052
§Present address: Naval Postgraduate School, Monterey, CA 93943.
‖Present address: National Science Foundation, Washington, D.C. 20550.
¶Present address: Taiwan Superconducting Cyclotron, Taiwan.
**Present address: CEBAF, Newport News, VA 23606.
††Present address: Woods Hole Oceanographic Institution, Woods Hole, MA 02543.

the two- and three-body breakup channels. The second uses bound and continuum Faddeev wave functions obtained for a simple central potential. Agreement with the data is good for the first model and better for the second. The inclusion of final-state interactions (FSI) in the Faddeev continuum is found to be very important in these threshold breakup kinematics; in many cases inclusion of FSI changes the response functions by factors of two or three giving excellent agreement with the data. The transverse response functions are well reproduced, even though neither model includes meson exchange currents. Ratios of the response functions for the two nuclei are also well described.

PACS number(s): 21.45.+v, 25.30.Fj, 27.10.+h, 25.10.+s

I. INTRODUCTION

While the ultimate goal of nuclear physics may be to describe real nuclei with a microscopic theory involving quarks and their interactions, there is much to learn with simpler, nucleons-only models. In these models the nucleus is described as a collection of nonrelativistic nucleons interacting through phenomenological potentials produced by boson (mainly pion) exchange. This model has been very successful in the past. A very important part of these models is often the interactions between the nucleons in the final-state interaction (FSI). The newest versions of these nucleons-only models also contain additional non-nucleonic degrees of freedom (DOF) such as meson-exchange currents (MEC), excitation of nucleonic resonances, three-body forces, or exchange of heavier bosons. Relativistic corrections have also been shown to be necessary. Addition of any of these non-nucleonic DOF generally improves the agreement between theory and the data.

For the $A = 2$ and 3 systems exact nonrelativistic calculations can be carried out for a given nuclear potential within the framework of the nucleons-only model. It is now possible to compute exact, nonrelativistic two- and three-body wave functions for both bound states and the continuum that also include some of the nonnucleonic DOF mentioned above. In particular, for the $A = 3$ case, Faddeev three-nucleon ground-state wave functions without the non-nucleonic DOF have been constructed for realistic nucleon-nucleon interactions. The differences between the theoretical predictions based on these wave functions and ground-state properties or the measured elastic electromagnetic form factors have been attributed to these non-nucleonic DOF. For inelastic scattering, FSI effects are expected to be important, but only a few calculations yet exist that attempt to properly treat the continuum with exact wave functions.

One recent attempt to treat the FSI between the outgoing nucleons is that of the Urbana group [1] in which two-body correlations are taken into account. Another calculation has been performed [2] using the Faddeev equation approach for different nucleon-nucleon interactions. A major difficulty for any of these calculations in the three-body breakup region is determining the solution of the three-body equations for the final state. The initial state consists of three off-shell nucleons and in the final three-body channel there are three on-shell nucleons. The calculation of these half off-shell scattering amplitudes for quasielastic scattering was reported by the Utrecht group [2]. In contrast to the quasielastic region, where relatively low-momentum components of the ground-state wave function are important, the threshold region should be sensitive to the high-momentum parts of the ground-state function because of the mismatch between energy and momentum transfer. In this paper, the Urbana and Utrecht calculations are compared to our threshold inelastic electron scattering data.

Our experiment is the first systematic study of the threshold region ($E_x = 0 - 18$ MeV excitation energy) of inelastic electron scattering cross sections on the mirror nuclei ^{3}H and ^{3}He. The longitudinal and transverse response functions R_L and R_T [see Eq. (1)] were obtained using Rosenbluth separations over an incident electron energy range of $100 < E_0 < 750$ MeV. The combination of incident energies and the scattering angles 54.0° and 134.5° resulted in momentum transfers in the range $0.88 < q < 2.87$ fm^{-1}. For both nuclei, we measured cross sections for the two-body breakup up to the three-body breakup threshold and beyond that the sum of the two- and three-body channels. The two- and three-body thresholds are $E_x = 5.4$ and 7.6 MeV, respectively, for ^{3}H and 6.2 and 8.4 MeV, respectively, for ^{3}H.

The ^{3}H(e,e') data presented here are the only measurements at this energy and momentum transfer. Existing inclusive ^{3}He electron scattering data [3–6] agree with the present measurements after scaling for the slightly different kinematics. Frosch *et al.* [3] searched for excited states in the threshold region at a single low q value. Chertok *et al.* [4] examined transverse scattering at 180° scattering angle. Kan *et al.* [5] measured the inclusive cross sections for between 0.3 and 1.1 fm^{-1} momentum transfer and up to 40-MeV excitation. Kobschall *et al.* [6] measured from threshold to beyond the quasielastic peak for $1.0 < q < 1.58$ fm^{-1}. An important aspect of our experiment was the measurement of both nuclei in the same experimental configuration. Thus, the ratios of our measured response functions are free from a number of experimental systematic uncertainties.

In the first Born approximation the most general unpolarized, in-plane, inclusive inelastic cross section can be written as [7]

$$\frac{d^2\sigma}{d\Omega d\omega} = \sigma_{\rm Mott}\left\{\frac{q_\mu^4}{q^4}R_L(q,\omega) + \left[\frac{q_\mu^2}{2q^2} + \tan^2\left(\frac{\theta}{2}\right)\right]R_T(q,\omega)\right\}. \quad (1)$$

The quantity $\sigma_{\rm Mott}$ is the Mott cross section for scattering from a point charge and $q_\mu^2 = \omega^2 - q^2 < 0$ is the

four-momentum transfer. The inelastic response functions were extracted from the experiment by using a q-ω grid interpolated from the actual data to adjust the measured cross sections to be at the same q and ω for both the forward and backward scattering angles. These cross sections were then substituted into Eq. (1) and R_L and R_T extracted. Such separations were performed at three-momentum transfers of 0.88, 1.28, 1.64, 2.08, 2.47, and 2.87 fm^{-1}. The response functions R_L and R_T correspond to reactions involving longitudinally and transversely polarized virtual photons, respectively. The response functions correspond to scattering from charge and current densities.

II. EXPERIMENTAL ARRANGEMENT

The data were taken using the 900-MeV/c energy-loss spectrometer system (ELSSY) at the MIT/Bates Linear Accelerator Center [8–11]. Two ferrite-toroid beam current monitors before the scattering chamber measured the total beam charge with an estimated uncertainty of 0.1%. Three identical cryogenic gas target cells were used for ^{3}H, ^{3}He or ^{1,2}H and the empty target. The cells were right circular cylinders whose axes were vertical and perpendicular to the beam direction. They were constructed of 0.127-mm-thick Elgiloy [13] foil brazed to two thick circular endplates and a stainless-steel filling line welded into the center of each top plate led to the gas supply systems. The cells (each containing two cryogenic temperature sensors) were cooled in series by a 70-W refrigerator. The gaseous tritium in the target cell amounted to 130 000 Curie; the safety equipment and procedures employed in the target system are discussed in Refs. [12,13].

The temperatures and pressures of the target gases and the average beam current were recorded in each event data block. Virial coefficients for ^{3}H and ^{3}He are not well known at our 45-K target temperature so we used the principle of corresponding states [14] to derive densities from gases whose coefficients are well known. The beam heating effect on the gas density was measured over the range of beam currents used during the experiment, and the appropriate corrections were applied off line. The systematic uncertainties in the densities were 2.1% for $^3H_2$ and 1.3% for the other gases, random uncertainties were 1.2%.

The ELSSY spectrometer [15] has point-to-point optics in the dispersion plane (9.66 cm/%) and parallel-to-point optics in the transverse plane. Two pairs of slits defined the solid-angle acceptance as well as the target length. The focal-plane instrumentation consisted of drift chambers with delay line readout to measure accurately the electron position in the dispersion direction. Another drift chamber measured the transverse position which is proportional to the scattering angle difference from the spectrometer central ray. This angle difference is used to correct for the kinematic broadening. This was followed by trigger scintillators and a gas Cherenkov detector for pion rejection. Event mode data were recorded onto magnetic tape for final analysis, and an on-line analysis of a subset of the data was used to monitor system performance. The absolute energy calibration for the spectrometer was obtained from an analysis of various elastic and inelastic levels obtained using a BeO target and a carbon target [7].

In the off-line analysis [11], empty target contributions were subtracted and the data corrected for various dead times and inefficiencies. Target densities were determined for each set of runs corresponding to a single fill of the sealed target cells. Energy-loss spectra were formed for each energy-angle combination, elastic radiation tails subtracted, and continuum radiative unfolding procedures were performed. The elastic tail subtraction was particularly important in the threshold region, and runs with a ^{1}H target (which has no inelastic contribution below pion threshold) verified the efficacy of the subtraction. The energy-loss spectra were then converted to final scattering cross sections as a function of excitation energy.

Deriving the response functions from the Rosenbluth equation [Eq. (1)] requires cross sections with identical q and ω, but at forward and backward scattering angles. A plot of $(q^2/q_\mu^2)^2(d^2\sigma/d\Omega_e dE')/\sigma_{\text{Mott}}$ vs $(q^2/q_\mu^2)^2[q_\mu^2/2q^2 + \tan^2(\theta_e/2)]$ gives a straight line having a slope R_T and a y intercept of R_L. Higher-order Feynman diagrams (multiple photon exchange, distortion of the electron plane wave by the static nuclear potential, vacuum polarization or virtual compton scattering, for example) would be indicated by the data following a curve rather than a straight line, for different θ. We have only two θ values and assume linearity (first Born approximation or one-photon exchange only) to extract the response functions. There is ample evidence that this is the case for light nuclei [10].

Data at the forward scattering angle were interpolated to produce a table of cross sections spanning the ω range; this process was then repeated for identical ω values for the backward scattering angle. The interpolated cross section values were then adjusted slightly to a common, average q value ($< 0.5\%$ different) for the two scattering angles. This was required since the initial energies shifted slightly in the off-line analysis and the q value no longer exactly matched. The statistical uncertainty in the response functions (shown in Figs. 2–4) were derived from the statistical uncertainties in the cross sections. No uncertainty was added to account for assumptions implicit in the derivation of the Rosenbluth equation.

III. RAW DATA AND SIMPLE MODELS

An example of the doubly differential inclusive cross section as a function of E_x is shown in Fig. 1. The data are all consistent with zero up to the two-body thresholds at 5.4 and 6.2 MeV for ^{3}He and ^{3}H, respectively. At these kinematics ($E_0 = 198.3$ MeV, $\theta_e = 54°$, $q = 0.88$ fm^{-1}) there is a clear shoulder in the ^{3}He cross section around 7–8 MeV which is not observed in ^{3}H. There is no significant point of inflection in the data at the energy where the three-body channel opens, 2.225 MeV above the two-body threshold. The overall systematic uncertainties in the cross sections are estimated at 5%. A complete set of

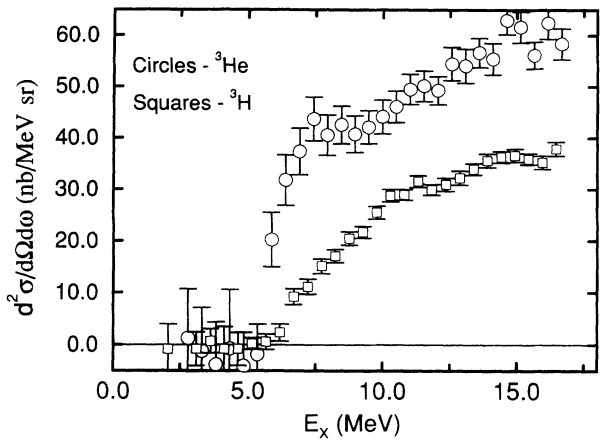

FIG. 1. Doubly differential inclusive scattering cross sections for $E_0 = 198.3$ MeV, 54°. Circles, ^{3}He data; squares, ^{3}H data.

our measured cross sections and derived response functions is tabulated in Ref. [11].

Figures 2–4 show the four response functions, R_L and R_T for each of ^{3}He and ^{3}H, at momentum transfers of 0.882, 1.64, and 2.47 fm^{-1}, respectively, three of the six momentum transfer values we measured. The structure functions are fairly consistent with zero until threshold is reached, however, not all data sets rise exactly at the thresholds due to uncertainty in the energy loss, see Fig. 2(d) in particular. These figures also contain the results of models discussed below. Again, no points of inflection are seen in the experimental data where the three-body channel opens, although some of the models show these.

A feature of these data is the presence of the enhancement near threshold in the ^{3}He but not in the ^{3}H longitudinal response function. This enhancement is more pronounced at lower q. The R_T response increases monotonically in this range of E_x. This enhancement was observed by Kan *et al.* [5] in their measured cross sections for ^{3}He. It was also observed by Kobschall *et al.* [6] in the longitudinal structure functions. By comparing their results to a zero-range approximation (ZRA) model, Kan *et al.* attributed the effect to a Coulomb $^2S \rightarrow {}^2S$ monopole ($C0$) longitudinal transition.

We extended the ZRA model to include ^{3}H, and calculated R_L for both nuclei. The ZRA ground-state (GS) wave function is the solution for a zero-range nuclear force whose depth is chosen to fit the ground-state binding energy and radius of the nucleus. The radial form of this wave function is exponential and has the proper asymptotic behavior. This ground state has been used to calculate $E1$ transitions in photodisintegration, where

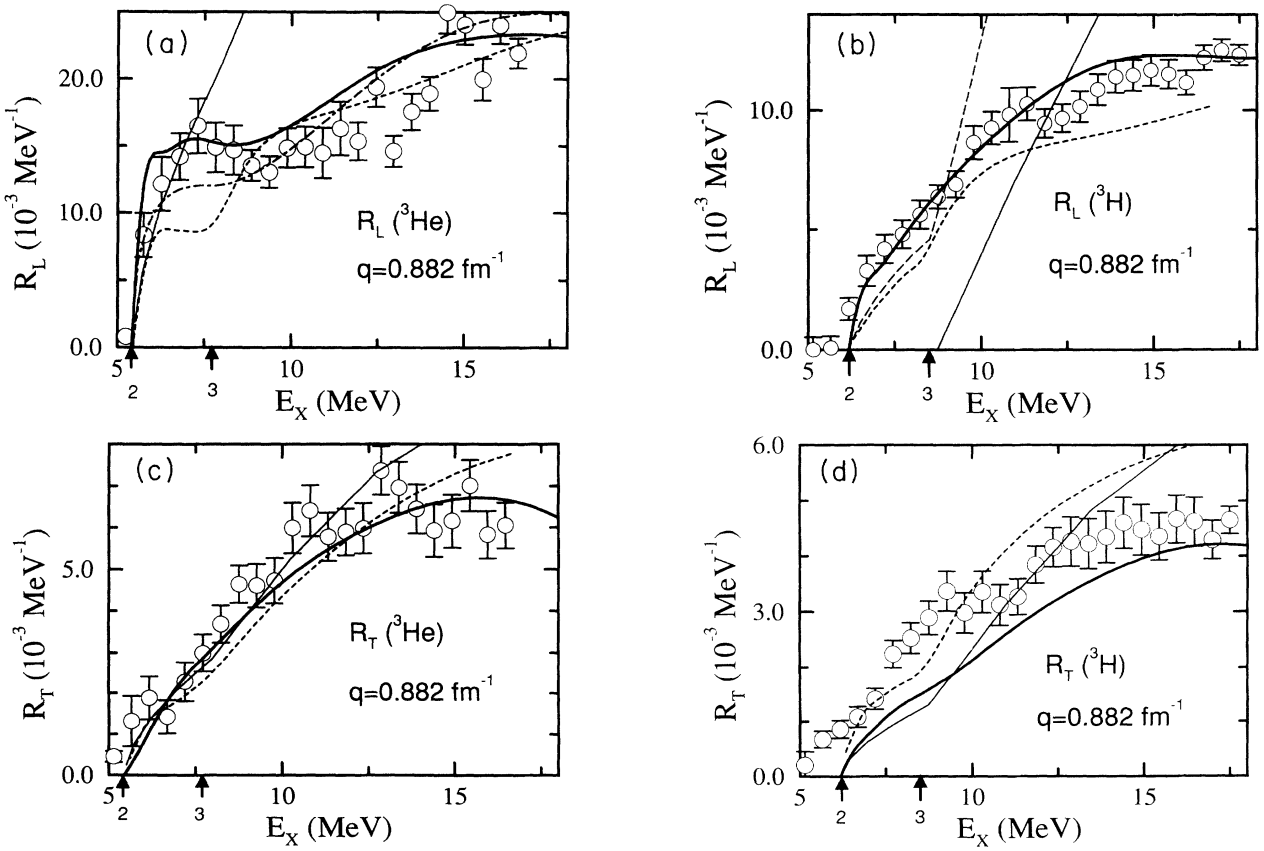

FIG. 2. ^{3}He longitudinal, (b) ^{3}H longitudinal, (c) ^{3}He transverse, and (d) ^{3}H transverse response functions, respectively, at $q = 0.882$ fm^{-1}. Circles, data; dot-dashed line ZRA (^{3}He longitudinal response only); long-dashed line, IG (^{3}H longitudinal response only); dashed line, OCS calculation; thin solid line, Utrecht PWIA; thick solid line, Utrecht total. The numbered arrows show the two- and three-body breakup thresholds.

the major contribution to the matrix element is at large r. Plane-wave final states were used, with the S-wave components shifted by the empirical nucleon-deuteron and nucleon-nucleon phase shifts, for the two- and three-body channels, respectively. Turning off this phase shift [11] affects the response functions by nearly a factor of 2 at some q values, suggesting the importance of FSI. Kan *et al.* found good agreement between this model and their data taken at relatively low-momentum transfers. However, as the momentum transfer increases, form factors based on this simple GS wave function are not expected to describe the data. We show the results of this simple ZRA model (dash-dotted line) only for the lowest- and highest-momentum transfers [Figs. 2(a) and 4(a)]. The ZRA result in Fig. 4(a) has been divided by five. At our lowest q (comparable to Kan's highest q value) we have fair agreement but as expected, the model fails to describe the data at the higher-momentum transfer.

Figure 5 shows that at low E_x, the $C0$ two-body breakup multipole dominates R_L for ^{3}He but not for ^{3}H. The ^{3}He and ^{3}H data are circles and squares, respectively. The long-dashed line is the ZRA calculation for ^{3}He with all multipoles, and the short-dashed line is the $C0$ multipole only. The solid and dot-dashed lines correspond, respectively, to all multipoles and $C0$ multipoles only, for ^{3}H. Heimbach, Lehman, and O'Connell [16] determined that this $C0$ enhancement in ^{3}He was caused by the constructive interference of the amplitudes in the two-body breakup of ^{3}He that corresponded to the virtual photon coupling directly to a proton or to a correlated proton-neutron pair. In ^{3}H, the virtual photon for the two-body breakup channel can couple only to the correlated pair since coupling directly to a proton leaves an unbound neutron pair and thus a three-body final state.

Another simple model was tried for R_L using slightly more realistic but still analytic wave functions consisting of a Hulthén deuteron wave function and an Irving-Gunn (IG) $A=3$ ground state. Final-state interactions were empirically included by using the nucleon-nucleon and nucleon-deuteron experimental phase shifts applied to the plane-wave final states. As with the ZRA, agreement with the data is fair at low q, worsening as q increases. Figure 2(b) shows an example of this calculation at low q (IG, long-dashed line). Both the ZRA and IG calculations give similar results and are especially poor in the three-body breakup region. For R_L at the lowest q, both these models show (at least qualitatively) the longitudinal $C0$ enhancement near 8-MeV excitation energy.

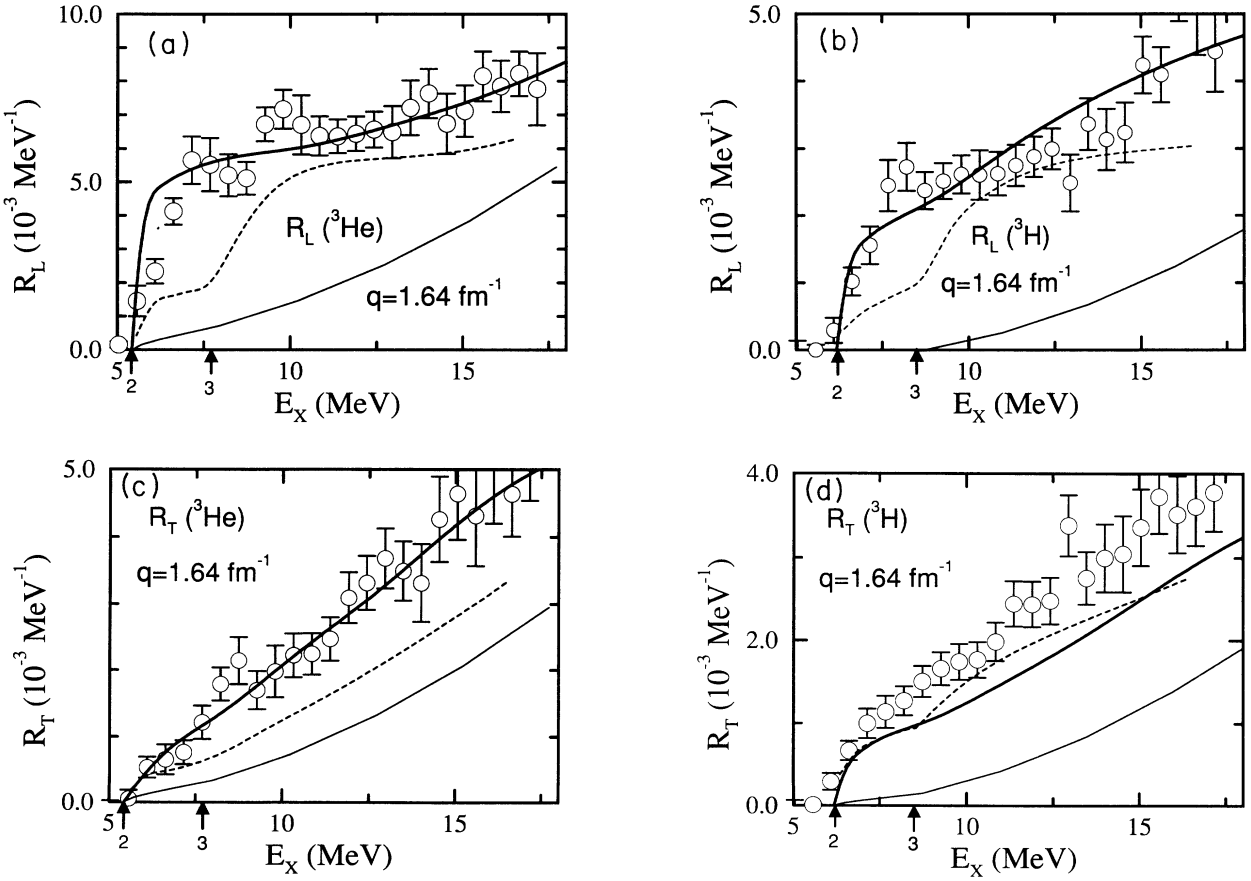

FIG. 3. (a) ^{3}He longitudinal, (b) ^{3}H longitudinal, (c) ^{3}He transverse, and (d) ^{3}H transverse response functions, respectively, at $q = 1.64$ fm^{-1}. Circles, data; dashed line, OCS calculation; thin solid line, Utrecht PWIA; thick solid line, Utrecht total. The numbered arrows show the two- and three-body breakup thresholds.

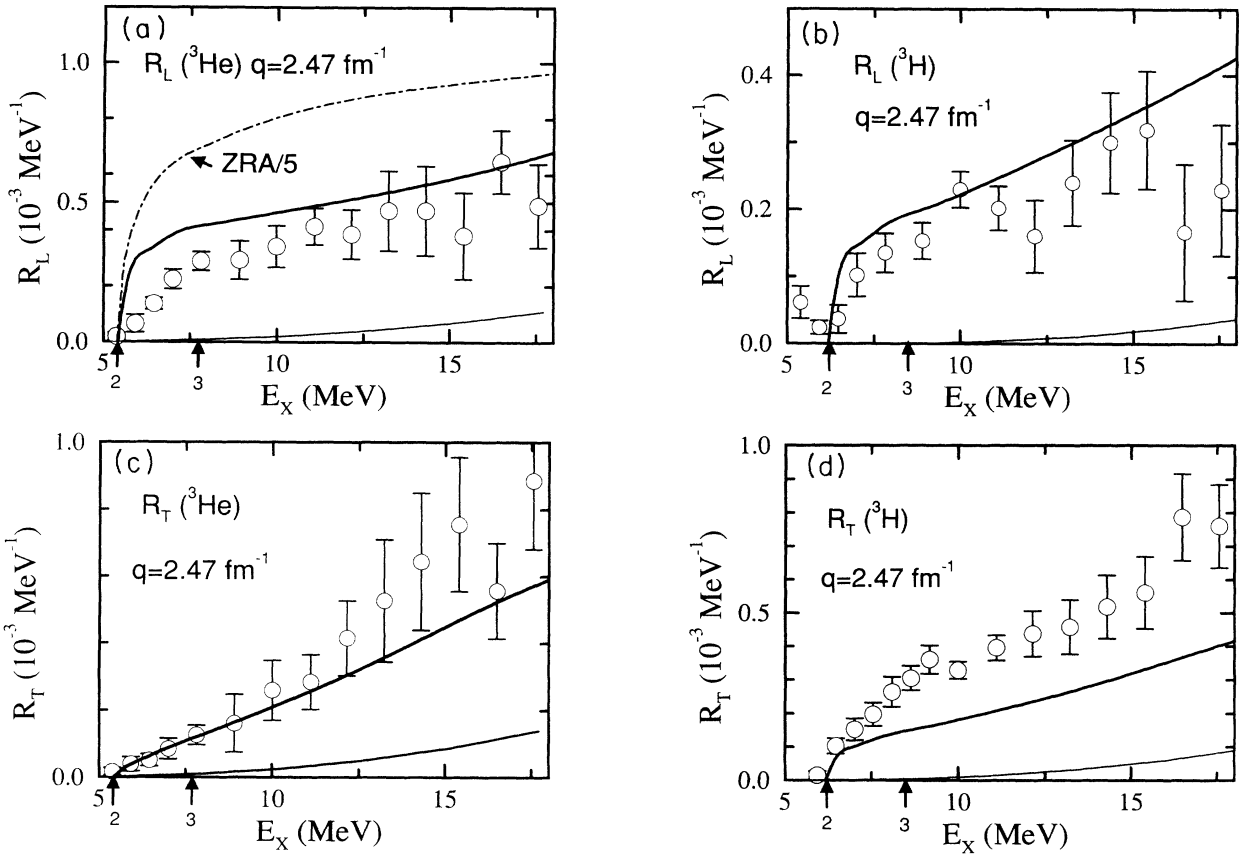

FIG. 4. (a) ^{3}He longitudinal, (b) ^{3}H longitudinal, (c) ^{3}He transverse, and (d) ^{3}H transverse response functions, respectively, at $q = 2.47\,\mathrm{fm}^{-1}$. Circles, data; dot-dashed line, ZRA/5 (^{3}He longitudinal response only); thin solid line, Utrecht PWIA; thick-solid line, Utrecht total. The numbered arrows show the two- and three-body breakup thresholds.

IV. MODERN TRINUCLEON MODELS

Other than simple models which use analytical wave functions, which we have seen to be deficient especially in the three-body breakup, the only two available calculations that make a serious attempt to treat the three-body continuum states are those of the Urbana [1] and Utrecht [2] groups. Both of these models have been applied to the quasielastic (QE) peak in the three-nucleon system [2,9]. The Urbana calculation gave only fair agreement with the QE data (within 30% or less of the data). The newer Utrecht calculation greatly improves the agreement at the QE peak by adding a more complete treatment of FSI effects using a Faddeev continuum final state, bringing theory into almost total agreement for three of the four responses [2], being consistently 5–10% below the data for the ^{3}H transverse response.

In the Urbana calculations, variational wave functions obtained from a realistic Hamiltonian with two- and three-nucleon interactions are used to describe the ^{3}H and ^{3}He ground states. The deuteron+nucleon and (nucleon+nucleon)+nucleon continuum wave functions are treated with the orthogonal correlated states (OCS) method developed in Ref. [1]. Some of the FSI's affecting the knocked-out nucleon in the two-body breakup channel are approximately taken into account by a deuteron+nucleon optical potential. Short-range correlations, orthogonality corrections, as well as FSI effects bring the calculated longitudinal and transverse response functions into reasonable agreement with all the data, as shown (OCS, dashed lines) in Figs. 2 and 3. In general, the agreement becomes somewhat poorer as q increases, but overall the model is a major improvement over the simple

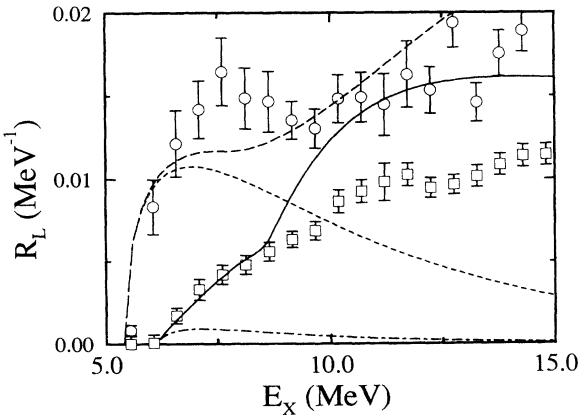

FIG. 5. Longitudinal response function at $q = 0.882$ fm^{-1} in the ZRA calculation. Long-dashed line, ^{3}He full calculation; short-dashed line, ^{3}He $C0$ two-body multipole only; solid line, ^{3}H full calculation; dot-dashed line, ^{3}H $C0$ two-body multipole only.

models discussed above. Qualitatively, the Urbana model also reproduces the $C0$ enhancement discussed above.

In the Utrecht calculation the Faddeev equations are solved exactly for the ground and the scattering states using the spin-dependent s-wave Malfliet-Tjon local nucleon-nucleon interaction. The resulting binding energy for the three-nucelon system is found to be 8.5 MeV, in reasonable agreement with the experiment. No Coulomb effects are included in these calculations, no tensor force is present, and the wave functions are nonrelativistic, although the kinematics are treated relativistically. To account for the different thresholds of ^{3}H and ^{3}He, the excitation energy is related to the center-of-mass energy of the three-nucleon system and is used to reconstruct the continuum wave functions. A reasonable description for inelastic scattering processes is expected as long as the initial momentum of the nucleon intially interacting with the exchanged virtual photon is limited to less than a few hundred MeV/c. However, when this model is compared to the data available in the quasielastic region [2], the transverse response is missing some strength, which may be due to MEC contributions that have not been included in this or the Urbana calculation.

The Utrecht results are shown in Figs. 2–4 [the light solid line is for plane-wave impulse approximation (PWIA) final state, the heavy solid line is the full calculation]. The agreement is excellent for most of our data. Only for the ^{3}H transverse response (where the calculation is ~25% below the data) is there a significant disagreement. This was also the case at the QE peak where the calculated transverse response for ^{3}H was consistently lower than the data. The difference between PWIA and the full calculation is large, in some cases an order of magnitude different. An interesting fact to note is that by adding a FSI, the QE peak response changes are relatively small (no more than ≈30%), while in the threshold region (see Figs. 2–4) much greater differences can be seen (often hundreds of percent). The PWIA is initially larger than the full calculation but becomes smaller than the full response as q increases. Only for the transverse response at the lowest-momentum transfer is the effect of FSI small [Figs. 2(c) and 2(d)]. If the data points in Fig. 2(d) were slightly shifted to reflect the correct threshold energy, agreement would be even better. Interestingly, the full calculation shows the $C0$ enhancement near threshold, while the PWIA does not.

The shape of the transverse response is well described by the Utrecht model, especially if the threshold excitation energy were free to vary slightly. Contributions from MEC to the response functions, which mainly effect the transverse response, have not been included in either model. The Utrecht calculation predicts the ^{3}He data almost exactly (especially at the lower q), although it consistently reproduces only about 75% of the measured response function for ^{3}H. It is unknown why one nucleus is well described, but not the other. The ^{3}He results imply that MEC are not very important or are cancelled out by other effects, while the ^{3}H results imply otherwise. One might expect the MEC effects would be proportional to the number of deuteron-like pairs, which is the same in ^{3}He and ^{3}H. The MEC are expected to become more important as q increases; indeed the agreement seems to worsen as q reaches our highest value. At the lowest q, there is little difference between the modern calculations.

Figures 6(a) and 6(b) show the ^{3}He/^{3}H ratios for each of the two response functions with the same labeling used in Figs. 2–4. We have subtracted the respective two-body threshold value E_2 (5.4 MeV for ^{3}He and 6.2 MeV for ^{3}H) from E_x to remove the effect of the different thresholds for each nucleus. This direct comparsion of the relative response of the two nuclei should cancel some experimental systematic uncertainties. In addition, some theoretical simplifications, such as the effects of nonrelativistic wave functions and problems in formulating a three-nucleon continuum wave function, may also cancel in the ratio. Both ratios (the transverse especially) flatten out for $E_x > 10$ MeV.

Both modern models do a credible job for the R_L ratio, especially at large excitation energies, while the simple models (not shown) are not as good. The transverse ratio calculations do not exactly agree with the data; in particular, the Utrecht calculation is worse than for the response functions alone which is an artifact of the consistently low ^{3}H transverse response noted above.

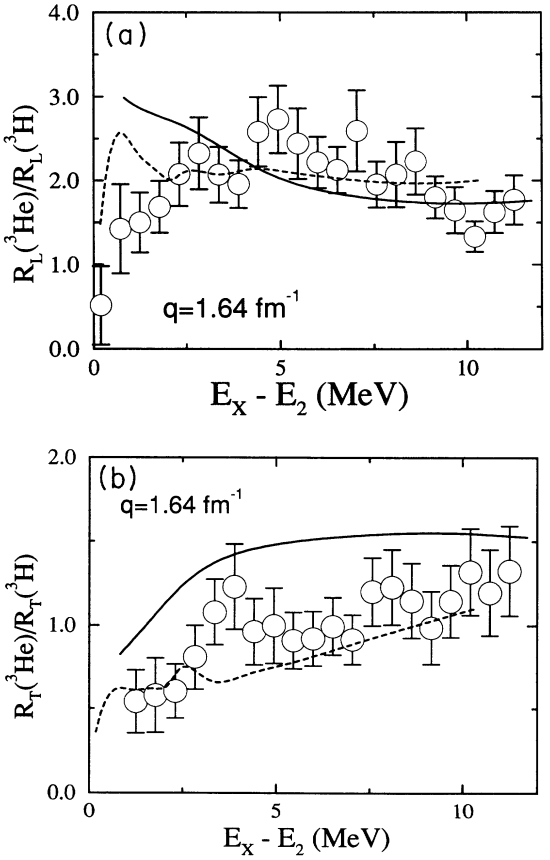

FIG. 6. ^{3}He/^{3}H ratios of response functions, for (a) longitudinal and (b) transverse. Circles, data; dashed line, OCS; heavy solid line, Utrecht total. The numbered arrows show the two- and three-body thresholds. The x axis is $E_x - E_2$ where E_2 is the two-body threshold for that nucleus.

The transverse ratio is quite close to unity in contrast to the dominance of ^{3}He over ^{3}H in R_L. At large excitation energies, the measured ratios flatten out and are close to that expected from simple considerations, where the transverse ratio is the ratio of the weighted sum of the squares of the nucleon magnetic moments $[(2\mu_p^2 + \mu_n^2)/(\mu_p^2 + 2\mu_n^2) = 1.27]$, and the longitudinal ratio expression, is similar, using the nucleon charges rather than the magnetic moments, yielding a ratio of 2 for the transverse response functions.

V. SUMMARY AND CONCLUSIONS

Threshold electron scattering response functions for ^{3}He and ^{3}H have been measured and compared to several models of the bound and unbounded three-nucleon system. The analytic ZRA and IG models yield fair agreement only in their expected range of applicability (low q), but do shed light on the characteristics of the $C0$ dominance in the two-body breakup near threshold. It is observed in both the data and these models that only for the R_L for ^{3}He is the response dominated by a $C0$ transition near threshold. Both of the modern models show indications of the $C0$ strength near threshold in ^{3}He. Overall the modern calculations, Urbana and Utrecht, give good agreement with the data. The Utrecht calculations agree almost eactly for R_L and the R_T for ^{3}He and gets about 75% of the observed strength for the R_T for ^{3}H. The remainder of our data, not illustrated in this paper, still agree well with the Utrecht calculation, but unfortunately no corresponding Urbana calculation has been performed for these other data. In the absence of MEC in the model, it is somewhat surprising (and perhaps fortuitous) that the calculation agreed so well with the measured transverse response functions. It is also not clear why the ^{3}He response agrees with the data while the ^{3}H response does not. The agreement for the transverse responses worsens as q increases, as one would expect from the MEC becoming more important as high-momentum transfer. The Utrecht theory demonstrates the tremendous influence of FSI in the threshold kinematics, which are much larger than the QE region. This is illustrated by the large difference between the full and PWIA calculations, with the FSI contributing most of the cross section at high q. Theory has predicted much less than the observed cross sections far from the QE peak (for example, see Ref. [9]), and speculation centered on larger than expected high-momentum parts of the ground-state wave function being responsible, or perhaps quark effects. According to the Utrecht calculation, this strength is caused by FSI.

In summary, by probing the threshold region of only slightly unbound nucleons, models of the interacting three-body system in scattering states, which, in principle, are calculable using continuum Faddeev methods, can be tested. Only now are these methods becoming tractable for realistic nucleon-nucleon potentials [17]. It is noteworthy that calculations of nucleon+deuteron three-body breakup cross sections and spin observables hint at the need for three-body forces [18]. Such forces are certainly expected at some level. Their need is also motivated by the inadequacy of conventional pairwise interaction calculations of the binding energies for $A = 3$ systems [19]. The present data, since they span such large-q range, should stimulate further tests of these continuum calculations and the underlying three-body dynamics.

ACKNOWLEDGMENTS

We wish to thank Dr. E. L. Tomusiak and G. Gryschuk of SAL for help with our calculations using analytic wave functions. This work was supported by the United States Department of Energy under Contract Nos. DE-AC05-84ER4-40150, DE-FG05-86ER4-0261, DE-AC02-76ER0-3069, the National Science Foundation under Contact Nos. PHY-85-05682, PHY-82-12214, and by the Canadian Natural Sciences and Engineering Research Council (NSERC).

[1] R. Schiavilla and V. Pandharipande, Phys. Rev. C **36**, 2221 (1987); R. Schiavilla, Phys. Lett. B **218**, 1 (1989).
[2] E. van Meijgaard and J. A. Tjon, Phys. Rev. C **45**, 1463 (1992); E. van Meijgaard, Ph.D. thesis, Rijksuniversiteit Utrecht, 1989.
[3] R. F. Frosch, H. L. Crannell, J. S. McCarthy, R. E. Rand, R. S. Safrata, L. R. Suelzle, and M. R. Yearian, Phys. Lett. **24B**, 54 (1967).
[4] B. T. Chertok, E. C. Jones, W. L. Bendel, and L. W. Fagg, Phys. Rev. Lett. **23**, 34 (1969).
[5] P. T. Kan, G. A. Peterson, D. V. Webb, Z. M. Szalata, J. S. O'Connell, S. P. Fivozinsky, J. W. Lightbody, and S. Penner, Phys. Rev. C **12**, 1118 (1975).
[6] G. Kobschall, E. Fein, C. Ottermann, K. Maurer, K. Rohrich, Ch. Schmitt, and V. H. Walther, Nucl. Phys. **A412**, 294 (1983).
[7] T. deForest and J. D. Walecka, Adv. Phys. **15**, 1 (1966).
[8] D. H. Beck *et al.*, Phys. Rev. Lett **59**, 1537 (1987); D. Beck, Ph.D. thesis, MIT, 1986.
[9] K. Dow *et al.*, Phys. Rev. Lett. **61**, 1706 (1988); K. Dow, Ph.D. thesis, MIT, 1987; T. S. Ueng, Ph.D. thesis, University of Virginia, 1988.
[10] T. Donnelly, *Symmetrics in Nuclear Structure*, Proceedings of the 1982 NATO Summer School (Plenum, New York, 1982).
[11] G. A. Retzlaff, Ph.D. thesis, University of Saskatchewan, 1988.
[12] Elgiloy Company, Elgin, Illinois 60121.
[13] G. A. Retzlaff, Nucl. Instrum. Methods B **24/25**, 950 (1987).
[14] J. O. Hirschfelder, C. F. Curtis, and R. B. Bird, *Molecular Theory of Liquids and Gases* (Wiley, New York, 1954), Chap. 4; J. H. Dymond and E. B. Smith, *The Virial Coefficients of Pure Gases and Mixtures* (Clarendon, New York, 1980); R. D. McCarty, *Selected Properties of Hydrogen*, Natl. Bur. Stand. (U.S.) Monograph No. 168 (U.S. GPO, Washington, D.C., 1981).
[15] W. Bertozzi *et al.*, Nucl. Instrum. Methods **141**, 457

(1977).
[16] C. R. Heimbach, D. R. Lehman, and J. S. O'Connell, Phys. Rev. C **16**, 2135 (1977).
[17] J. L. Friar, B. F. Gibson, and G. L. Payne, Annu. Rev. Nucl. Sci. **34**, 403 (1984); W. Glockle, H. Witala, and Th. Cornelius, Nucl. Phys. **A508**, 115c (1990), and references therein.
[18] W. Meier and W. Gloeckle, Phys. Lett. **138B**, 329 (1984); J. L. Friar (private communication).
[19] E. Hadjimicheal, Nucl. Phys. **A508**, 161c (1990); B. Gibson, *ibid.* **A513**, 1c (1993).